Monogalactosyldiacylglycerol and digalactosyldiacylglycerol role, physical states, applications and biomimetic monolayer films

Javier Hoyo[1,*], *Ester Guaus*[1], *Juan Torrent-Burgués*[1]

[1]*Universitat Politècnica de Catalunya, Group of Molecular and Industrial Biotechnology, Dpt. Chemical Engineering, 08222 Terrassa (Barcelona), Spain*

*Corresponding autor: javier.hoyo@upc.edu. Colom 1, E-08222 Terrassa (Barcelona), Spain, Tlf: +34 937398953.

Abstract

The relevance of biomimetic membranes using galactolipids has not been expressed in an extensive experimental study of these lipids. On the one hand, we present an intensive literature work about the presence and role of monogalactosyldiacylglycerol (MGDG) and digalactosyldiacylglycerol (DGDG) in thylakoid membranes, their physical states and their applications. On the other hand, we use the Langmuir and Langmuir-Blodgett (LB) techniques to prepare biomimetic monolayers of saturated galactolipids MGDG, DGDG and MGDG:DGDG 2:1 mixture (MD) -biological ratio-. These monolayers are studied using surface pressure – area isotherms and their data are processed to light their physical states and mixing behaviour. These monolayers, once transferred to a solid substrate at several surface pressures are topographically studied on mica using atomic force microscopy (AFM) and using cyclic voltammetry for studying the electrochemical behaviour of the monolayers once transferred to indium-tin oxide (ITO), which has good optical and electrical properties. Moreover, MD present other differences in comparison with its pure components that are

explained by the presence of different kind of galactosyl headgroups that restrict the optimal orientation of the MGDG headgroups.

Keywords

monogalactosyldiacylglycerol, digalactosyldiacylglycerol, galactolipids, biomimetic membrane, Langmuir-Blodgett film, modified ITO electrode.

Abbreviations

AFM	Atomic Force Microscopy
ATP	Adenosine triphosphate
C_d	Differential capacitance
CV	Cyclic voltammogram
DGDG	Digalactosyldiacylglycerol
ITO	Indium-tin oxide
LB	Langmuir-Blodgett
LC	Liquid Condensed state
LE	Liquid Expanded state
L_α	Liquid-crystalline state
L_β	Lamellar gel
L_c	Lamellar crystalline
MD	MGDG:DGDG 2:1 mixture
MGDG	Monogalactosyldiacylglycerol
PG	Phosphatidylglycerol
S	Solid state

SPB Supported planar bilayer

SQDG Sulfoquinovosyldiacylglycerol

1. Introduction

Lipid membranes can self-organize and interact with biomolecules, both at its surface and within the membrane, due to the amphiphilic character and electrostatic charge of the lipid components [1,2]. Supported planar bilayer (SPB) or monolayers onto solid surfaces are widely used as model for mimicking biological membranes. The resulting biomimetic membranes have been obtained with good reproducibility, stability, robust behaviour, fluidity and lateral mobility. In addition, its composition is tuneable including the insertion of proteins, nanoparticles and other entities [3,4].

Biomimetic membranes have been prepared previously using several model lipids [2-4] but rarely using galactolipids that are the main component of plant membranes. Monogalactosyldiacylglycerol (MGDG) (Fig. 1A) is a galactolipid that has a headgroup of 1-β-galactose linked to the diacylglycerol, whereas digalactosyldiacylglycerol (DGDG) (Fig. 1B) has the same structure to MGDG although presenting the headgroup a terminal α-galactose (1→6) linked to the inner β-galactose. Both galactolipids have two acyl groups esterified at the sn−1 and sn−2 positions of the glycerol moiety and the polar headgroup at the sn−3 position [5, 6]. The molecular motion of both galactolipids depends on the number of unsaturations in the alkyl chains [7] that is determined by the fatty acid desaturase enzymes activity [8].

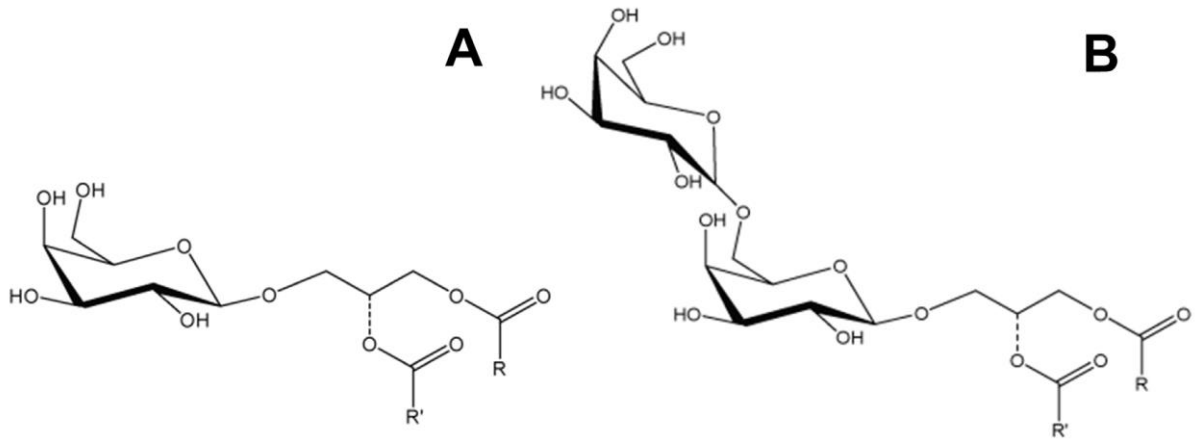

Figure 1. Scheme of a molecule of (A) MGDG and (B) DGDG.

We understand that the relevance of biomimetic membranes using galactolipids requires an extensive study of these lipids. In this work we use Langmuir and Langmuir-Blodgett (LB) techniques to prepare biomimetic monolayers of MGDG, DGDG and MGDG:DGDG 2:1 (MD) -MD ratio present in natural plant membranes-, due to the high control over the membrane structure that the LB technique confers compared with other techniques for biomimetic membrane formation [9]. These monolayers are studied using surface pressure – area, π-A, isotherms and their data are processed to light their physical states and mixing behaviour. These monolayers, once transferred to a solid substrate at several surface pressures (including the lateral pressure of natural membranes ≈ 33 $mN \cdot m^{-1}$ [10]) will be topographically studied on mica using atomic force microscopy (AFM) and cyclic voltammetry for studying the electrochemical behaviour of the monolayers once transferred to indium-tin oxide (ITO). This substrate has good optical and electrical properties, so converting it in a good candidate for studying artificial photosynthesis and other energy producing devices [11]. In addition, an intensive literature work has been performed to present information about the presence and role of galactolipids in thylakoid membranes, their physical states and their applications.

1.1 MGDG and DGDG presence and functions in thylakoid membranes

The thylakoid membrane of chloroplasts of oxygenic organisms is the site where the photochemical and electron transport reactions of photosynthesis take place. This thylakoid membrane is constituted by a lipid matrix that avoids the free diffusion of ions, maintains the fluidity of the membrane and allows an electrochemical potential difference across this membrane, which is required for ATP synthase [5]. The 70% of the thylakoid membrane area is occupied by proteins and the remaining 30% is mainly constituted by lipids. The lipid content of the thylakoid matrix depends on the plant and its external conditions. However, it can be agreed that higher plants are composed by the following lipids: MGDG (≈ 50%), DGDG (≈ 30%), sulfoquinovosyldiacylglycerol (SQDG) (≈ 5-10%), phosphatidylglycerol (PG) (≈ 5-10%) [7] and small amounts of other lipids [6,12]. The acyl chains of higher plants are polyunsaturated whereas other photosynthetic organisms are monounsaturated or fully saturated [13].

The outer envelope of chloroplast is principally composed by bilayer-forming lipids such as DGDG and phosphatidylcholines, being this zone relatively permeable [14]. On the other hand, the inner envelope is composed of non-bilayer forming lipids such as MGDG and phosphatidylethanolamine. The cone shape of MGDG, with a galactose at the tip and the two fatty acyl chains oriented towards the base of the cone, leads to hexagonal type-II (H_{II}) regions, whereas the cylindrically shaped DGDG, SQDG and PG forms convex structures in aqueous environments [12,15]. Thylakoid membranes of photosynthetic organisms increases the ratio of non-bilayer/bilayer forming lipids and the unsaturation index to adapt the fluidity and the related functions to changes in external temperature or to an increase in the protein:lipid ratio that can occur during greening [16-18].

The lipids present in thylakoid membranes can be classified in three groups depending on their function in the membrane: i) lipids that forms the bilayer matrix; ii) lipids that surround the protein-cofactor supercomplexes and interact with the outer surface of the complexes, and iii) integral lipids that are embedded in protein-cofactor supercomplexes. MGDG and DGDG are present in all the three groups, and in addition, their content is involved in the targeting of proteins to and within the chloroplast and in the generation of lipid signalling molecules [19]. Tthe presence of both lipids is essential for the development of thylakoid membranes and the stabilization of photosynthetic proteins [5], although DGDG is not an essential component for the cell growth [20,21]. DGDG binds extrinsic proteins that stabilize the oxygen evolving complex and stimulate the oxygen evolution in Photosystem II core complex, which induce changes in the protein structure [22,23]. DGDG is important for the function of the light harvesting complex II [6,24] and its deficiency restricts intersystem electron transport [5,12,20]. More information about the role of MGDG is still not possible due to hindrances on preparing MGDG-lacking mutants [5].

MGDG is assembled in the inner envelope of the membranes and it is exported to the thylakoid membrane [25], whereas DGDG is naturally synthesized by dismutation of two MGDG molecules thanks to the DGDG synthase localized in the outer envelope [26]. It is interesting to point that DGDG has not been found outside organisms with oxygenic photosynthesis [27]. For more detailed biosynthesis information of thylakoid lipids the reader is addressed to the following articles [28, 29].

1.2 MGDG and DGDG physical states

MGDG

Unsaturated MGDG -in the liquid-crystalline state (L_α)- forms a mesophase in aqueous solution in which molecules aggregate in inverted tube-like structures of infinite length in hexagonal arrays, which are called H_{II} structure with the polar head groups facing towards the centre. On the other hand, saturated MGDG forms sheet-like (lamellar) bilayers in the same conditions [30,31]. Gounaris et al. [32] found that 0.5 double bonds per molecule of MGDG induce the conversion of lamellar phase to H_{II} structure and increasing the unsaturation index, the transition temperature of the lamellar phase to H_{II} is decreased [16].

The presence of double bonds in MGDG displaces the control for the molecules order from hydrophobic interactions between lipid chains to be leaded by the stabilization of the headgroups [13,19]. It has been observed that the introduction of the first unsaturation in a saturated lipid influences in a high extent the compact packing, but the introduction of the subsequent unsaturations does not decrease the packing in a proportionate mode [13].

Lamellar gel (L_β) phase of saturated MGDG is metastable at 20ºC when formed by cooling from the L_α. The chains are arranged in hexagonal packing, but the heads present two spacings. After some minutes, the phase undergoes spontaneously to lamellar crystalline (L_c) in which the chains pack on orthorhombic subcell and the heads occupy a hexagonal spacing. The rearrangement of the chains into a more closely packed subcell is produced thanks to the reorientation of the heads to reduce the steric hindrance [33]. On the other hand, the fully hydrated and unsaturated MGDG forms H_{II} phase, which after cooling undergoes L_α state through cubic phase as intermediate. The reduction of the water content favours a direct transition from lamellar to H_{II} phase [34].

Saturated MGDG presents L_β to L_α transition at ≈ 80ºC [35]. On the other hand, unsaturated and hydrated MGDG forms nonlamellar structures such as cubic or H_{II} phase over a wide range of temperature (≈ -15 to 80°C) [36]. The L_β to H_{II} transition for unsaturated MGDG with similar unsaturation index has been studied in several conditions, being ≈ 32ºC in pure aqueous solution [36], ≈ 29ºC in aqueous buffered solution [37] and ≈ 84ºC in dry samples [34].

The ability of unsaturated MGDG to form non-lamellar structures like H_{II} can be neutralized when mixing it with at least 50% of bilayer forming lipids [14,34,38], although unsaturated MGDG induces regions of deformation in the lamellar structure of MGDG:bilayer-forming lipid when the presence of unsaturated MGDG is between 20 and 50 mol%. Conversely, the H_{II} structure can be favoured by dehydration, either through the removal of water or the addition of electrolytes [34].

DGDG

Conversely to MGDG, DGDG forms lamellar sheets and liposomes in the L_α state in aqueous solution regardless the saturation index [14,30,39]. The cone shape of unsaturated MGDG permits the formation of more curved zones so favouring smaller liposomes than DGDG that forms larger liposomes with larger trapped volume [14]. Saturated DGDG presents L_β to L_α transition at ≈ 55ºC [35]. On the other hand, a fully hydrated DGDG bilayer in lamellar phase has a height of ≈ 5.5 nm that can decrease up to 4.5 nm when reducing the hydration level [19].

1.3 Galactolipids applications

Galactolipids show several biological activities and they have been proposed as anti-algal, anti-viral, anti-tumor and anti-inflamatory agents. MGDG and DGDG have potential anticancer

functions due to DNA polymerase inhibition, suppression of cancer cell proliferation, anti-angiogenesis and anti-tumor promotion properties [40-43]. Indeed, glycolipid fraction of spinach has shown anti-tumor activity with oral administration in colon tumor in mice. Moreover, it has been observed that the hydrolized form of biological glycolipids, in particular hydrolized MGDG, has more anti-tumor activity than the non-hydrolized form [41]. DGDG and, in particular, MGDG have an important anti-inflamatory activity, which is reduced when increasing the saturation index [40]. On the other hand, DGDG has also been proposed for controlling the appetite [44].

2. Materials and methods

2.1 Materials

MGDG and DGDG, with acyl = stearoyl (18:0), were purchased from Matreya (USA). KH_2PO_4, KCl and chloroform of analytical grade from Sigma-Aldrich were used in solutions preparation. Water was ultrapure MilliQ® (18.2 MΩ·cm and surface tension 72.2 $mN \cdot m^{-1}$). Mica sheets were purchased from TED PELLA Inc (CA) and ITO deposited on glass slides were purchased to SOLEMS (France).

2.2 Methods

2.2.1 Monolayer formation

Langmuir and Langmuir-Blodgett monolayer formation were carried on a trough (Nima Technology, Cambridge, UK) model 1232D1D2 equipped with two movable barriers. The surface pressure was measured using paper Whatman 1 held by a Wilhelmy balance connected to a microelectronic system registering the surface pressure (π).

The subphase used in these experiments was fresh MilliQ® quality water. Previous to the subphase addition, the trough was cleaned twice with chloroform and once with MilliQ® quality water. Residual impurities were cleaned from the air|liquid interface by surface suctioning. The good baseline in the π–A isotherms confirms the interface cleanliness. Stock solutions (maximum 1 week) of MGDG, DGDG, and MD were prepared using chloroform and kept at -20ºC until one hour before starting the experiment, and then kept at room temperature during experiments. 120 µL of the 500 $mg \cdot mL^{-1}$ stock solution was spread at the air|liquid interface using a high precision Hamilton microsyringe. LB monolayers were transferred to mica surface at defined surface pressure values. Barrier closing rates were fixed at 50 $cm^2 \cdot min^{-1}$ for isotherm registration and at 25 $cm^2 \cdot min^{-1}$ for LB film transfer. No noticeable influence of these compression rates was observed on the isotherm shape. Isotherm recording was carried out adding the solution to the subphase and lagging 15 minutes for perfect spreading and solvent evaporation. LB film transfer was conducted dipping the freshly cleaved mica or freshly cleaned ITO through the air|liquid interface on the subphase before adding the solution, and five minutes were lagged after pressure setpoint was achieved. LB films were obtained by the vertical dipping method (emersion), resulting in a film with the galactolipid polar groups oriented towards the ITO hydrophilic surface. Transfer speed was set at 5 $mm \cdot min^{-1}$ linear velocity. The deposition ratio was ca. 70% before the physical state change and ca. 100% after this event. Experiments were conducted at 21±1ºC and repeated a minimum of three times for reproducibility control.

2.2.2 AFM characterization

The AFM topographic images of LB films were acquired in air tapping mode using a Multimode AFM controlled by Nanoscope IV electronics (Veeco, Santa Barbara, CA) under

ambient conditions. Triangular AFM probes with silicon nitride cantilevers and silicon tips were used (SNL-10, Bruker), which have a nominal spring constant ≈ 0.35 $N \cdot m^{-1}$. Images were acquired at 1.5 Hz and at minimum vertical force so as to reduce sample damage. AFM images were obtained from at least two different samples, prepared on different days, and by scanning several macroscopically separated areas on each sample. AFM images have been obtained from LB films transferred at several surface pressures, being the rationale before and after the physical state change and the biologically relevant π = 33 $mN \cdot m^{-1}$.

2.2.3 Electrochemical characterization

Voltammetric measurements were performed in a conventional three-electrode cell using an Autolab Potentiostat-Galvanostat PGSTAT-12 (Ecochemie, NL). Working electrodes were freshly-cleaned ITO slides (10 mm x 25 mm), cleaned once with ethanol and three times with MilliQ® grade water. Counter electrode was a platinum wire in spiral geometry and the reference electrode was an Ag/AgCl/3M KCl microelectrode (DRIREF-2SH, World Precision Instruments). This reference electrode was mounted in a Lugging capillary containing KCl solution at the same cell concentration. All reported potentials were referred to this electrode. The electrochemical cell contained 0.150 M KCl as supporting electrolyte at pH 7.4 adjusted with the KH_2PO_4/K_2HPO_4 buffer solution. All solutions were freshly prepared with MilliQ® grade water de-aerated with a flow of Ar gas for 15 min prior to the cyclic voltammetry (CV) experiments that were conducted at 21±1ºC. Voltammetric experiments were carried out at several scan rates, scanning towards cathodic potentials in a homemade glass cell with a reaction area of 33 mm^2.

3. Results

3.1 π-A isotherms, physical states and mixing behaviour

The π-A isotherms of MGDG, DGDG and their mixture (MD) at biological relevant ratio MGDG:DGDG 2:1 are presented in Fig. 2. Inset of Fig. 2 represents the inverse of the compressibility modulus (C_s^{-1}) curves corresponding to the described π-A isotherms, and they are calculated according to Eq. 1.

$$C_s^{-1} = -A\left(\frac{d\pi}{dA}\right)_T \tag{1}$$

The most significant values of Fig. 2 are summarized in Table 1.

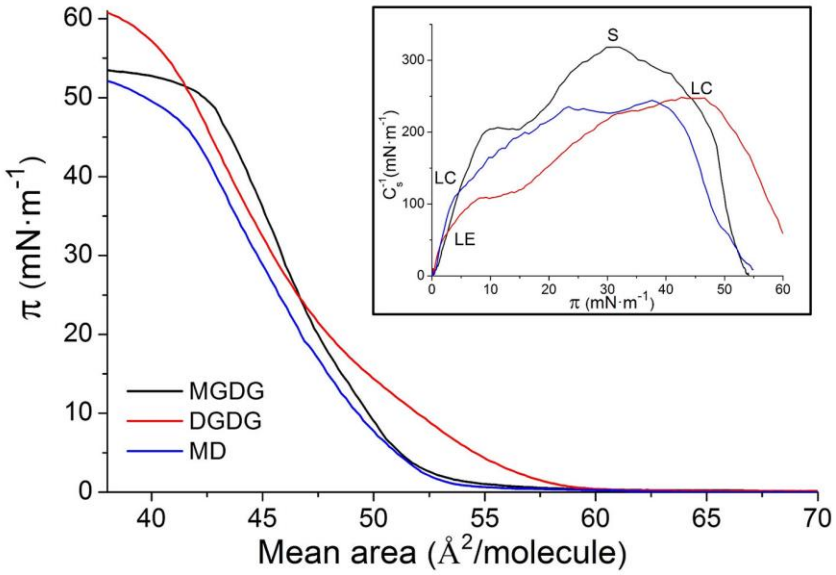

Figure 2. π-A isotherms for MGDG, DGDG and MD at 21 ± 1 ºC on water subphase. Inset: Inverse of the compressibility modulus *vs*. surface pressure for the same systems.

Table 1. Lift-off area, limiting area and collapse pressure for MGDG, DGDG, MD from Fig. 2.

	Lift-off area ($Å^2 \cdot molecule^{-1}$)	Limiting area ($Å^2 \cdot molecule^{-1}$)	Collapse pressure ($mN \cdot m^{-1}$)	$C_s^{-1}{}_{max}$ ($mN \cdot m^{-1}$)
MGDG	59	49	53	320
DGDG	59	51	57	249
MD	57	51	49	247

In order to understand the interactions present in our system, it is interesting to compare the results obtained using our saturated galactolipid with the results for saturated or unsaturated galactolipid found in the literature. The explanation is that the shape of the galactolipid π-A isotherm and $C_s^{-1}{}_{max}$ value depends strongly on the unsaturation index of the acyl chains.

3.1.1 MGDG

The saturated MGDG lift-off area is substantially different than the 80-100 $Å^2 \cdot molecule^{-1}$ observed by Tomoaia-Cotişel et al. [13,33]. However, the limiting area and collapse pressure observed in our results coincides with their observations. The lift-off area is found at 95-120 $Å^2 \cdot molecule^{-1}$ for an unsaturation index below the unity, whereas the limiting area for the same experiments is found at 45 $Å^2 \cdot molecule^{-1}$ [31] for an unsaturation index of ≈ 0.2 and at ≈ 75 $Å^2 \cdot molecule^{-1}$ for an unsaturation index ≈ 0.8 [31,45]. MGDG in pure water or buffered solution using TRIS at pH 8 with an unsaturation index ≈ 2.7 presents the lift-off area at 140 $Å^2 \cdot molecule^{-1}$ and a limiting area ≈ 91 $Å^2 \cdot molecule^{-1}$ [46,47] whereas in the same conditions but pH 7 using phosphate [48], these areas are reduced to 120 and 82 $Å^2 \cdot molecule^{-1}$ respectively. On the other hand, Bottier et al. [19] using NaCl electrolyte as subphase and MGDG with an unsaturation index ≈ 2 presents a limiting area of 82 $Å^2 \cdot molecule^{-1}$. The results [46,47] obtained at an unsaturation index ≈ 2.7 indicate that the presence or absence of the

buffer ions has no effect on the isotherm for unsaturated MGDG whereas the reduction of only one unit of pH reduces ≈ 10 % the lift-off and the limiting area. It is also important that, comparing the experiments using NaCl electrolyte [19] with the pure water subphase [46,47], the presence of hydrated ions of the electrolyte produce an expansion of the monolayer compared with pure water subphase [13].

Looking at the collapse surface pressure, the value observed for saturated MGDG is higher than that for unsaturated MGDG found in the literature, being the later independent of the unsaturation index and experimental conditions. In pure water and unsaturation index below the unity, the collapse pressure is ≈ 42 $mN \cdot m^{-1}$ [31,45,49] being this value close to the ≈ 43 $mN \cdot m^{-1}$ obtained with an unsaturation index ≈ 2.7 in pure water [47], phosphate [48] or TRIS buffered solution at pH 7-8 [46,50]. In addition, Bottier et al. [19] observed the collapse at 46 $mN \cdot m^{-1}$ using NaCl electrolyte subphase with 2 unsaturations.

Accordingly to the values presented by Vitovic et al. [51] our MGDG presents liquid-condensed (LC) phase from low surface pressures till the solid (S) state formation at $\pi \approx 10$ $mN \cdot m^{-1}$ (inset of Fig. 2) where a plateau is observed until $\pi \approx 15$ $mN \cdot m^{-1}$ indicating phase change to S state (more detailed information about the physical state for the studied galactolipids) is presented in section 3.2). Unsaturated MGDG on water subphase presents a $C_s^{-1}{}_{max}$ of ≈ 39 $mN \cdot m^{-1}$ [31] and ≈ 35 $mN \cdot m^{-1}$ [31,45] for an unsaturation index of 0.2 and 0.8 respectively. The use of TRIS buffered solution at pH 7.4 enhances the $C_s^{-1}{}_{max}$ for a 0.4 unsaturation index to 54 $mN \cdot m^{-1}$ [52], presenting unsaturated MGDG liquid-expanded (LE) state in all the studied conditions.

3.1.2 DGDG

Saturated DGDG lift-off area (59 $Å^2 \cdot molecule^{-1}$) and collapse pressure (57 $mN \cdot m^{-1}$) observed in our experiments differs substantially to those observed using similar conditions by Tomoaia-Cotişel et al. [13] (85 $Å^2 \cdot molecule^{-1}$ and 67 $mN \cdot m^{-1}$) whereas the limiting area observed in our results coincides with their observations. The differences may be attributed to the method used for DGDG purification and/or the presence of impurities and the different solvent used for DGDG solution preparation.

Looking at the lift-off area reported in the literature, DGDG with a 0.6 unsaturation index presents the mentioned area at 100 $Å^2 \cdot molecule^{-1}$ [31], and increasing the unsaturation index to 1-1.3, this area is 105-125 [31,49]. In water at 37 ºC and 2.6 unsaturations per molecule, the lift-off area is observed at 165 $Å^2 \cdot molecule^{-1}$ [44]. Moreover, DGDG with 1.7 unsaturations per molecule in water with NaCl electrolyte as subphase shows a lift-off area of 135 $Å^2 \cdot molecule^{-1}$ [19] and DGDG with 1 unsaturation in TRIS buffered subphase at pH 7.4 marks this area at 120 $Å^2 \cdot molecule^{-1}$ [52]. On the other hand, Gzyl-Malcher et al. [31] found that the limiting area for DGDG with 0.6 unsaturation index is 52 $Å^2 \cdot molecule^{-1}$. Increasing the unsaturation index to 1, the area is 80-90 [31,45,49] and 101 $Å^2 \cdot molecule^{-1}$ with an unsaturation index of 1.3 [49]. In water at 37 ºC and 2.6 unsaturations per molecule, the limiting area is observed at 125 $Å^2 \cdot molecule^{-1}$ [44]. Experiments in other subphases, like DGDG with 1.7 unsaturations per molecule in water with NaCl electrolyte presents the limiting area at 64 $Å^2 \cdot molecule^{-1}$ [19] and DGDG with 1 unsaturation in TRIS buffered subphase at pH 7.4 shows this area at 95 $Å^2 \cdot molecule^{-1}$[52]. These last results confirm that the presence of hydrated ions of the electrolyte also produce an expansion of the monolayer compared with the pure water subphase, whereas the presence of electrolytes does not affect the collapse pressure [13].

There is strong consensus in the collapse pressure for unsaturated DGDG regardless the conditions employed. In water subphase and similar temperature the collapse pressure was observed at 46-47 $mN \cdot m^{-1}$ with 0.6-1.3 unsaturations per DGDG molecule [31,45,49]. In water at 37 ºC and 2.6 unsaturations per molecule, the collapse was observed at 43 $mN \cdot m^{-1}$ [44]. Moreover, DGDG with 1-1.8 unsaturations in water with NaCl electrolyte subphase or in TRIS neutral pH subphase presents the collapse at 43-46 $mN \cdot m^{-1}$ [19,52,53].

Our DGDG presents LE phase from low surface pressure till the compact state formation at $\pi \approx 8$ $mN \cdot m^{-1}$ (inset of Fig. 2) where a plateau is observed until $\pi \approx 15$ $mN \cdot m^{-1}$ indicating phase change to LC state. The compression of the saturated DGDG monolayer forces the reorientation of the heads favouring the formation of hydrogen bonds between DGDG molecules, which is reflected in an increase of the compressibility of the monolayer [33] compared with MGDG. The presence of unsaturations in the alkyl chain of the DGDG molecule affects in a large extend the $C_s^{-1}{}_{max}$. This is the case reported by Gzyl-Malcher et al. [31] who observed $C_s^{-1}{}_{max} \approx 64$ $mN \cdot m^{-1}$ for an unsaturation index of 0.6 and increasing the unsaturation index to 1, the $C_s^{-1}{}_{max}$ is minored to 54 $mN \cdot m^{-1}$.

3.1.3 MD

At the best of our knowledge, saturated MD has never been studied, so we compare our results with the scarce literature for unsaturated MD. MD in water subphase with an unsaturation index of ≈ 0.2 shows the lift-off and limiting area at 55 $Å^2 \cdot molecule^{-1}$ and 50 $Å^2 \cdot molecule^{-1}$ respectively [31] whereas for an unsaturation index of ≈ 0.8, these areas are placed at 100 $Å^2 \cdot molecule^{-1}$ and 75 $Å^2 \cdot molecule^{-1}$ respectively [31,45]. The unsaturated MD mixture in NaCl

electrolyte subphase and unsaturation index of ≈ 2 [19] presents the lift-off and the limiting area at 150 $Å^2$·molecule^{-1} and 70 $Å^2$·molecule^{-1} respectively. On the other hand, the collapse pressure for the unsaturated MD mixture in water is ≈ 43 mN·m^{-1} for an unsaturation index lower than the unity [31,45]. In NaCl electrolyte subphase and unsaturation index of ≈ 2, the collapse pressure observed is 47 mN·m^{-1}[19].

Inset of Fig. 2 shows that MD presents LC phase during the entire isotherm. The MD mixture presents a $C_s^{-1}{}_{max}$ value of ≈ 247 mN·m^{-1} closer to that of DGDG rather than MGDG, being this behaviour explained by the most fluid component leads the mixture compactness. The $C_s^{-1}{}_{max}$ for unsaturated MD on water subphase has been observed at ≈ 47 mN·m^{-1} [31] and ≈ 40 mN·m^{-1} [31,45] for an unsaturation index of 0.2 and 0.8 respectively, both presenting LE state.

The excess area (Eq. 2) for the MD isotherm is negative at several surface pressures, which indicates that MGDG and DGDG form non-ideal mixtures with negative deviation at the entire range of surface pressures, which can indicate more favourable interactions between MGDG and DGDG molecules due to the similar cylindrical shape of both galactolipids.

$$A^E = A_{12} - (x_1 A_1 + x_2 A_2) \quad (2)$$

Where A^E is the excess area, A_{12} the mean area per molecule for the mixture. A_1 and A_2 the area per molecule for the individual components and x_1 and x_2 the molar fraction of each component.

The literature shows that unsaturated MD mixtures form non-ideal monolayers at the air|water interface and exhibits strong tendency towards phase separation although remain miscible, in particular, at MGDG:DGDG molar ratio similar to our experiments at which the non-attractive interactions between MGDG and DGDG are the weakest [31,45]. In our saturated MD mixture,

the more favourable interactions suggested by the absence of an inflexion in the MD isotherm and the high similarities between saturated MGDG and DGDG pure components suggest the favourable mixing behaviour previously to the collapse.

3.1.4 Comparison between MGDG, DGDG and MD.

The $C_s^{-1}{}_{\max}$ values (inset of Fig. 2) indicate that MGDG presents LC phase at low surface pressure, which undergoes S state at high surface pressure, whereas MD presents mostly LC during the entire isotherm. On the other hand, DGDG presents LE and LC at low and high surface pressure respectively. These results indicate that DGDG presents more fluid states than MGDG that also affects MD in which the presence of DGDG hindrances the formation of the S state despite of the high MGDG content.

The lower collapse pressure and the larger lift-off and limiting area observed for unsaturated galactolipid monolayers compared with our saturated galactolipid results were expected. The headgroups are the same so they produce similar interactions in both saturated and unsaturated, whereas the presence of these unsaturations in the galactolipid chains hindrances the tighter packing for both heads and tails [54] and the intensity of the van der Waals forces between them. Besides the presence of unsaturations, their position in the alkyl chain determine the area and volume occupied by the galactolipid molecule and therefore, influencing the compactness of the monolayer [14]. The high collapse pressure and the low limiting area observed for saturated galactolipid is a clear sign that two cooperative forces are involved. First, the hydrophilicity of the galactolipid heads governs the packing, so reducing the distances between galactolipid chains thanks to the formation of hydrogen bonds. Second, these chains are completely saturated so the van der Waals forces between the hydrocarbon chains are favoured and therefore, enhancing the compactness and the stability of the monolayer.

The comparison between saturated and unsaturated of the same galactolipid confirms that an increase in the unsaturation index of the acyl chains provokes a reduction of the monolayer $C_{s\ \max}^{-1}$. In particular, the first unsaturation which produces a decrease of $C_{s\ \max}^{-1}$ values from ≈ 320 to 39 mN·m^{-1} for MGDG, ≈ 249 to 64 mN·m^{-1} for DGDG and ≈ 247 to 40 mN·m^{-1} for MD.

It is interesting to point that there are also differences in the alkyl chain length between the galactolipids used in the exposed experiments of several authors, but the small differences in hydrophobic interactions are largely overcome by the double bond hindrance in the monolayer stability. The low value of $C_{s\ \max}^{-1}$ for unsaturated galactolipids confirms that, conversely to saturated galactolipid, they present LE phase from its appearance in the G-LE phase coexistence till the collapse [19,44,46,48,52]. The presence of unsaturations in the galactolipid chains extends the LE phase due to hindrances for a tight packing, even forbidding the formation of the LC state. The different orientations that can be adopted by the sugar moiety of MGDG depend on the hydrogen bonds established [19,38]. Bottier et al. [19] observed that in an unsaturated MGDG:DGDG mixture, the MGDG headgroup forces the DGDG head to a different orientation than in pure DGDG monolayers, and that the presence of both galactolipids induced a higher hydration than in pure components. In our case, the absence of unsaturations permits chains of both lipids to compete with the heads for leading the packing.

3.2 AFM

Fig. 3 presents AFM topographic images corresponding to the studied galactolipids transferred at several surface pressures on mica, including π = 33 mN·m^{-1} that is the internal lateral surface pressure of natural cell membranes [10]. Most of the images present two tonalities of brown

(fair and dark), and in addition, images A, C and F also present a medium brown tonality. The observation of different brown tonalities is related with different monolayer height, which is correlated with different tilting of the galactolipid molecules, so presenting a different physical state. It is important to remark that each brown tonality indicates a different height but the physical state that is correlated with them depends on the surface pressure at which the monolayer has been transferred.

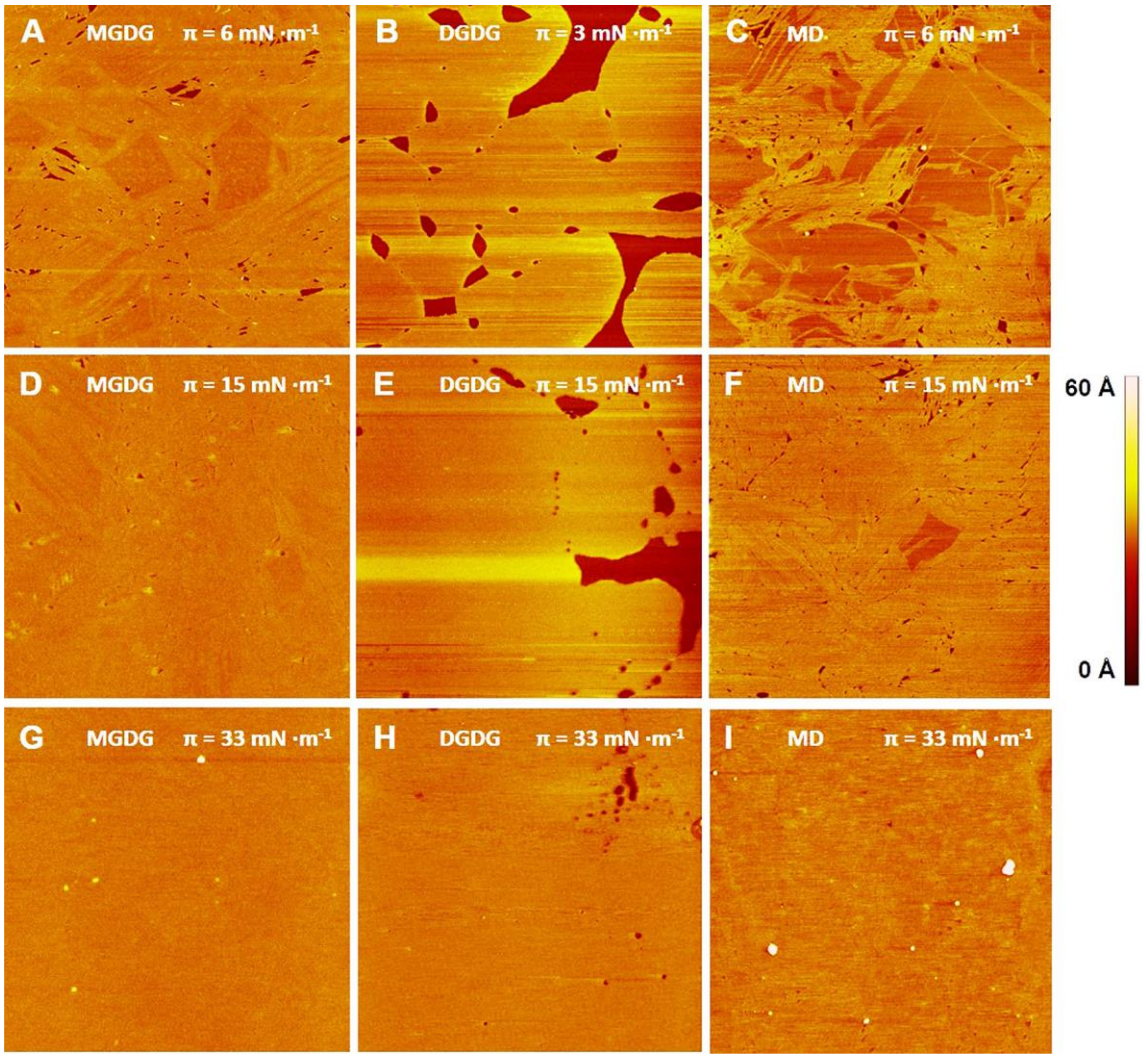

Figure 3. AFM images (5µm x 5µm) for LB films of the studied galactolipids transferred on mica at several surface pressures at 21ºC.

The low relative height between dark brown zones referred to medium or fair brown zones and the 100% LB transfer ratio indicate that dark brown zones corresponds to a physical state of the galactolipid monolayer. The presence of dark brown zones at low surface pressures and the

reduction of the area occupied by them when increasing the surface pressure indicate that these zones are in fluid state. Moreover, if we observe the values of $C_s^{-1}{}_{max}$ presented in section 3.1, we deduce that these zones are in LE state. On the other hand, we can estimate the height of the LE zones based on previous works of the authors [55,56], in which mixed monolayers of galactolipid-plastoquinone (PQ) were studied. In those works, the presence of $\approx 15\%$ of PQ content in the mixed monolayer induces hole defects in the LE state that arrive to the mica surface, which allowed us to measure the LE height (6 ± 2 Å). This height is in accordance to the 3-6 Å observed in the literature for LE of DPPC [57,58]. So that, accepting that this value should be close to that of pure galactolipid, we calculate the absolute height of each physical state (Table 2) according to it and the relative heights previously measured. On the other hand, the presence of medium and fair brown tonalities (images A, C and F) cannot be correlated with the presence of zones in S state due to the isotherms and the $C_s^{-1}{}_{max}$ values presented in section 3.1 does not point this option. So that, we correlate both tonalities to LC state, being LC1, corresponding to molecules in the beginning of the LC state (medium brown), and LC2, molecules at the most ordered state of the LC state (fair brown). Table 3 presents the physical state that corresponds to fair and dark brown tonality in Fig.3.

Table 2. Height of each physical state for the LB monolayers of MGDG, DGDG, MD on mica.

*Estimated value (more information in the text).

	LE	LC1	LC2	S
MGDG	6 ± 2 *	21 ± 1	25 ± 1	27 ± 1
DGDG	6 ± 2 *	21 ± 1	24 ± 1	
MD	6 ± 2 *	21 ± 1	25 ± 1	

Table 3. Physical states of each zone (dark and fair brown) corresponding to MGDG, DGDG and MD at several surface pressures.

	MGDG		DGDG		MD	
π (mN·m^{-1})	Dark	Fair	Dark	Fair	Dark	Fair
3 or 6	LE	LC2	LE	LC1	LE	LC2
15	LC1	LC2	LC1	LC2	LE	LC2
33	-	S	LC1	LC2	LC1	LC2

The compression of the monolayers leads to the ordering of the LE phase transforming it gradually in LC, and in the MGDG case at high surface pressure, in S state. The remaining small LE or LC1 areas at medium-high surface pressure achieve rounded shape (Images D, F, H, I). On the other hand, the surface pressure at which the most compact state covers the entire mica surface depends on the galactolipid nature. As it can be observed in Fig. 3 at $\pi = 33$ mN·m^{-1} the solid state of MGDG covers the entire mica surface, whereas DGDG presents ≈ 2% of the monolayer in LC1 state. As it was expected, MD presents a behaviour comprised between MGDG and DGDG, presenting only 0.5% of the monolayer in LC1 state. DGDG on mica at low surface pressures ($\pi \leq 3$ mN·m^{-1}) forms round edge domains of a compact state (Image B) whereas the compact state of MGDG and MD form amorphous shapes. We correlate this observation with the different nature of the galactolipid heads. On the other hand, the similarity between MD and MGDG is correlated to the high MGDG content in the MD mixture.

Our observations for saturated MGDG, DGDG and MD differs to the Bottier et al. [19] work using unsaturated galactolipids. They observed homogeneous LE phase images with no visible phase separation at several surface pressures. In addition, they observed irregular protrusions of ≈ 7 Å at $\pi > 25$ mN·m^{-1} for the MGDG and rounded protrusions of ≈ 4 Å with a diameter of ≈100 nm at $\pi > 25$ mN·m^{-1} for the MD. They attributed these protrusions to a specific

organization of the monogalactosyl headgroups due to strong lateral interactions between themselves and between them and the DGDG headgroups in the MD case. The flatten disks sometimes observed in our AFM images seem to have no relation with the lower protrusions observed by Bottier et al. [19] that covers an important area of the monolayer. Using our saturated galactolipids no segregation, no protrusions are observed even at high surface pressure, so that, the different behaviour is correlated with the absence of double bonds.

Although some white undefined shape zones (higher than the monolayer) are also seen at low surface pressure when MGDG is present, the compact monolayers of the studied galactolipids present at medium-high surface pressure some rounded shape structures that increase in number when increasing the surface pressure. The origin of such structures is uncertain but we hypothesize that they are the result of a local surface pressure increase, which induces a local collapse [59,60] of the film, forming flatten disks of 100 - 250 nm diameter and height of 0.5 to 20 nm. These observations are consistent with small flatten bilayer vesicles, in line with previous observations for POPG [61] and DPPG [62]. In the particular case of MD, the presence of the two different galactolipids facilitates the formation of local tensioned zones, which explains the existence of these flatten disks even at low surface pressure.

The lower collapse pressure observed for MD compared with pure MGDG and DGDG can be explained by the formation of the presented white rounded shape structures which, once formed, hindrance the perfect packing of the remaining molecules at the air|water interface, so facilitating the collapse. The slightly lower limiting area observed for MD is also related with the formation of these structures, which provoke the lost of molecules at the galactolipid|water interface so reducing the number of molecules and their stability at this region so inducing a higher compression.

3.3 Electrochemical behaviour

Fig. 4 shows the cyclic voltammogram (CV) at a scan rate of 10 $mV \cdot s^{-1}$ of LB films of MGDG, DGDG and MD transferred on ITO in a 0.150 M KCl cell solution buffered at pH 7.4. LB films have been transferred according to the criterion of being the monolayer at the most compact state for each galactolipid. Monolayers have also been transferred at a less ordered physical state (not shown), presenting a similar shape and differential capacitance (C_d) (Inset of Fig. 4) to those observed in Fig. 4.

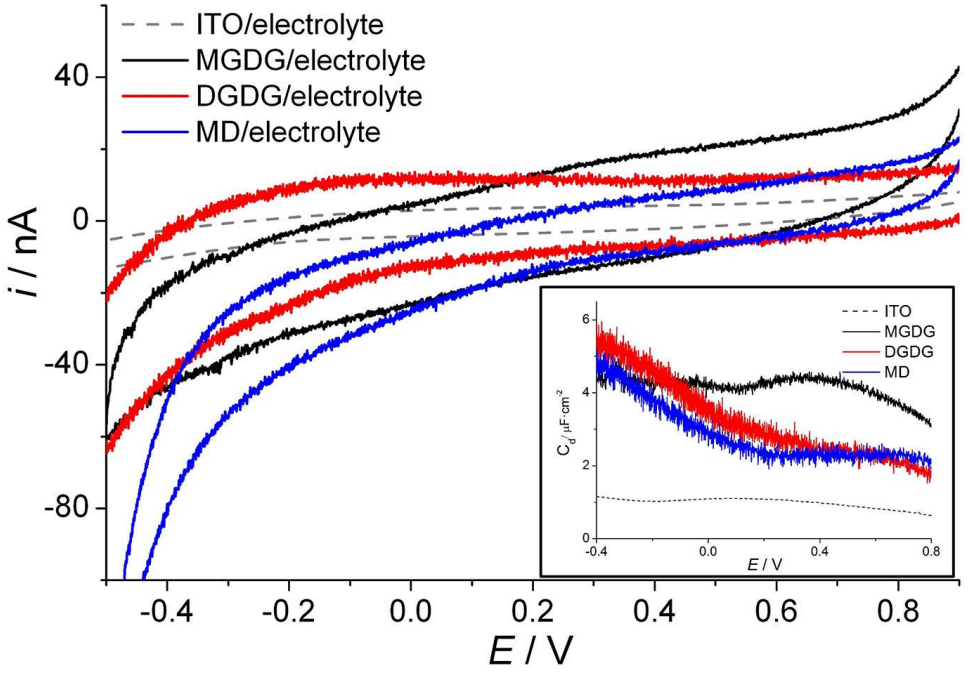

Figure 4. Cyclic voltammograms of the ITO/electrolyte, ITO-MGDG/electrolyte, ITO-DGDG/electrolyte and ITO-MD/electrolyte system with the galactolipid monolayers transferred at π = 33 $mN \cdot m^{-1}$ that is the internal lateral surface pressure of natural cell membranes. Inset: C_d obtained from the CVs presented in Fig. 4.

C_d is obtained from the value of the voltammetric charging current [9] (Eq. 3) where i_a and i_c are the capacitive current for anodic and cathodic scan respectively, v the scan rate and A_w the electrode area.

$$C_d = \frac{(i_a - i_c)}{2vA_w} \quad (3)$$

It has been observed that ITO behaves as a polarizable electrode in the experimental conditions, so no faradaic current is observed in the working potential window of 1.00 to -0.70V (see dashed line in Fig. 4) presenting a C_d around 1 $\mu F \cdot cm^{-2}$, in line with the literature [9,63,64].

Three CVs are required to obtain the stationary state in the electrochemical response of ITO-galactolipid/electrolyte systems, presenting a good reproducibility from the third scan and at least 15 cycles. CVs indicate that in the potential range between 0.80 and -0.40 V ITO-MGDG, ITO-DGDG and ITO-MD electrodes do not show faradaic response and the effect of the applied electrical potential on the lipid monolayer is low. For the ITO-MGDG and ITO-DGDG systems, a continuous increase (not shown) of the current intensity was obtained at more cathodic potentials than -0.40 V, indicating hydrogen evolution. For the ITO-MD system, the increasing of the current intensity starts at -0.20 V, which is correlated with a higher permeation of water molecules for the MD mixture than for the pure MGDG and DGDG monolayers, in line with the conclusions of Bottier et al. [19] using PM-IRRAS. On the other hand, the reproducible behaviour of the CVs indicates that the lipid layer is permeable to water molecules, and after the third scan, the stable water content is achieved in the monolayer. This effect, and its reversibility, of the applied potential on galactolipid LB monolayers on ITO are explained by the galactolipid heads-ITO affinity [65].

ITO-MGDG electrode presents a constant $C_d \approx 4$ $\mu F \cdot cm^{-2}$ in the potential window studied, whereas ITO-DGDG electrode presents an increasing C_d from 2 to 5.5 $\mu F \cdot cm^{-2}$ and the ITO-MD electrode presents an increasing C_d from 2 to 4.5 $\mu F \cdot cm^{-2}$ when scanning from 0.80 to -0.40 V. All ITO-galactolipid/electrode systems present higher C_d values than bare ITO. C_d values ≈ 1.8 $\mu F \cdot cm^{-2}$ have been reported for high quality lipid monolayers [66], so indicating that our monolayer is not completely homogeneous and presents few defects. Owing to the higher compactness of MGDG compared with DGDG and MD, it presents a more stable C_d value when changing the applied potential, even in the case of monolayers transferred at low surface pressures.

4. Conclusions

MGDG and DGDG present the coexistence of two different physical states during a wide range of surface pressures, being LE and LC in the case of DGDG and LC and S for MGDG, whereas MD presents mainly LC state. On the other hand, the similarities in the lift-off area between MGDG and DGDG are also maintained in the MD mixture, although the collapse pressure is lower than that of both components. This observation is explained by the presence of different kind of galactosyl headgroups that restrict the optimal orientation. Once transferred to the mica surface, the galactolipid monolayer present zones with different height, which is correlated with a different tilting of the galactolipid molecules that corroborates the coexistence of different physical states.

ITO-galactolipid electrodes present slightly higher C_d values than that reported for high quality lipid monolayers, so indicating that galactolipid monolayers are not completely homogeneous and present few defects. MGDG presents a more stable C_d value when changing the applied

potential in comparison with DGDG and MD, which is correlated with the higher compactness of its physical state.

Acknowledgements

The authors thank the economic support of the Spanish Government, through the project CTQ2007-68101-C02, and of the Catalonia Autonomic Government, through the project SGR2009-277. J Hoyo thanks to Universitat Politècnica de Catalunya its PhD grant.

Author contribution

All authors have equally contributed to the present article.

5. References

[1] H.Gao, G.Luo, J.Feng, A.L.Ottova, H. Ti Tien. Photoelectric conversion properties of bilayer lipid membranes self-assembled on an ITO substrate. J. Electroanal. Chem. **496**, 158 (2001).

[2] D.Berti, G.Caminatia, P.Baglioni. Functional liposomes and supported lipid bilayers: towards the complexity of biological archetypes. Phys. Chem. Chem. Phys. **13**, 8769 (2011).

[3] E.T.Castellana, P.S.Cremer. Solid supported lipid bilayers: From biophysical studies to sensor design. Surface Science Reports **61**, 429 (2006).

[4] R.Guidelli, G.Aloisi, L. Becucci, A. Dolfi, M.R. Moncelli, F. Tadini Buoninsegni. New directions and challenges in electrochemistry. Bioelectrochemistry at metal/water interfaces. J. Electroanal. Chem. **504**, 1 (2001).

[5] N.Mizusawa, H.Wada. The role of lipids in photosystem II. Biochim Biophys Acta **1817**, 194 (2012).

[6] P.Dörmann, G.Hölzl. in: Wada, Hajime; Murata, Norio (Eds.) Essential and Regulatory Functions, The Role of Glycolipids in Photosynthesis. Springer, Dordrecht, The Netherlands, 265 (2010).

[7] C.Glöckner. The donor and acceptor side of photosystem II: Structural and functional investigations. Ph.D. thesis, Technischen Universität Berlin, Berlin, 2013.

[8] D.A.Los, N.Murata. Structure and expression of fatty acid desaturases. Biochim Biophys Acta **1394**, 3 (1998).

[9] J.Hoyo, E.Guaus, G.Oncins, J.Torrent-Burgués, F.Sanz. Incorporation of Ubiquinone in Supported Lipid Bilayers on ITO. J. Phys. Chem. B **117**, 7498 (2013).

[10] G.Cevc, D.Marsh. Phospholipid Bilayers. Physical Principles and Models. Wiley-Interscience, New York, 1987.

[11] S.Morandat,K. El Kirat. Cytochrome c provokes the weakening of zwitterionic membranes as measured by force spectroscopy. Colloids Surf. B **82**, 111 (2011).

[12] A.G.Ivanov, L.Hendrickson, M.Krol, E.Selstam, G.Oquist, V.Hurry, N.P.Huner. Digalactosyldiacylglycerol deficiency impairs the capacity for photosynthetic inter-system electron transport and state transitions in Arabidopsis thaliana due to photosystem I acceptor-side limitations. Plant Cell Physiol. **47**, 1146 (2006).

[13] M.Tomoaia-Cotişel, J.Zsakó, E.Chifu, P.J.Quinn. Influence of electrolytes on the monolayer properties of saturated galactolipids at the air-water interface. Chemistry and Physics of Lipids **34**, 55 (1983).

[14] A. A.Foley, A.P.R.Brain, P.J.Quinn, J.L.Harwood. Permeability of liposomes composed of binary mixtures of monogalactosyldiacylglycerol and digalactosyldiacylglycerol. Biochim. Biophys. Acta **939**, 430 (1988).

[15] D.Marsh. Components of the lateral pressure in lipid bilayers deduced from HII phase dimensions. Biochim. Biophys. Acta **1279**, 119 (1996).

[16] T.Páli, G.Garab, L.I.Horváth, Z.Kóta. Functional significance of the lipid-protein interface in photosynthetic membranes. Cell Mol Life Sci. **60**, 1591 (2003).

[17] N. Murata. Low-temperature effects on cyanobacterial membranes. J. Bioenerg. Biomemb. **21**, 61 (1989).

[18] T.Mock, B.M. Kroon. Photosynthetic energy conversion under extreme conditions-II: the significance of lipids under light limited growth in Antarctic sea ice diatoms. Phytochemistry **61**, 53 (2002).

[19] C.Bottier, J.Géan, F.Artzner, B.Desbat, M.Pézolet, A.Renault, D.Marion, V.Vié. Galactosyl headgroup interactions control the molecular packing of wheat lipids in Langmuir films and in hydrated liquid-crystalline mesophases. Biochim Biophys Acta **1768**, 1526 (2007).

[20] I.Sakurai, N.Mizusawa, H.Wada, N.Sato. Digalactosyldiacylglycerol is required for stabilization of the oxygen-evolving complex in photosystem II. Plant Physiol. **145**, 1361 (2007).

[21] A.A.Kelly, J.E.Froehlich, P.Dörmann. Disruption of the two digalactosyldiacylglycerol synthase genes DGD1 and DGD2 in Arabidopsis reveals the existence of an additional enzyme of galactolipid synthesis. Plant Cell **15**, 2694 (2003).

[22] K.Gounaris, D.Whitford, J.Barber. The effect of thylakoid lipids on an oxygen-evolving photosystem II preparation. FEBS Lett. **163**, 230 (1983).

[23] M.Fragata, A.Menikh, E.K.Nénonéné. Functional and structural aspects of the thylakoid lipids in oxygen evolution in photosystem II. Trends Photochem. Photobiol. **3**, 201 (1994).

[24] H.Wada, N.Mizusawa. in: Wada, Hajime; Murata, Norio (Eds.) Essential and Regulatory Functions, The Role of Phosphatidylglycerol in Photosynthesis. Springer, Dordrecht, The Netherlands, 243 (2010).

[25] A.Rawyler, M.Meylan-Bettex, P.A.Siegenthaler. (Galacto)lipid export from envelope to thylakoid membranes in intact chloroplasts. II. A general process with a key role for the

envelope in the establishment of lipid asymmetry in thylakoid membranes. Biochim. Biophys. Acta **1233**, 123 (1995).

[26] P. Dörmann. Functional diversity of tocochromanols in plants. Planta **225**, 269 (2007).

[27] G. Hölzl, P. Dörmann. Structure and function of glycoglycerolipids in plants and bacteria. Prog Lipid Res **46**, 225 (2007).

[28] L.Boudière, C.Botte, N.Saidani, M.Lajoie, J.Marion, L.Bréhélin, Y.Yamaryo-Botté, B.Satiat-Jeunemaître, C.Breton, A.Girard-Egrot, O.Bastien, J.Jouhet, D.Falconet, M.A.Block, E.Maréchal. Galvestine-1, a novel chemical probe for the study of the glycerolipid homeostasis system in plant cells, Mol. Biosyst. **287**, 22367 (2012).

[29] N.Rolland, G.Curien, G.Finazzi, M.Kuntz, E.Marechal, M.Matringe, S.Ravanel, D.Seigneurin-Berny. The biosynthetic capacities of the plastids and integra-tion between cytoplasmic and chloroplast processes. Annu. Rev. Genet. **46**, 233 (2012).

[30] A.Sen, A.P.Brain, P.J.Quinn, W.P.Williams. Formation of inverted lipid micelles in aqueous dispersions of mixed sn-3-galactosyldiacylglycerols induced by heat and ethylene glycol. Biochim. Biophys. Acta **686**, 215 (1982).

[31] B.Gzyl-Malcher, M.Filek, K.Makyła, M.Paluch. Differences in surface behaviour of galactolipids originating from different kind of wheat tissue cultivated in vitro. Chem Phys Lipids **155**, 24 (2008).

[32] K.Gounaris, A.Sen, A.P.R.Brain, P. J.Quinn, W. P.Williams. The formation of non-bilayer structures in total polar lipid extracts of chloroplast membranes. Biochim. Biophys. Acta **728**, 129 (1983).

[33] M.Tomoaia-Cotişel, J.Zsako, E.Chifu, P.J.Quinn. Hysteresis in compression-expansion cycles of distearoylmonogalactosylglycerol monolayers. Chem. Phys. Lipids **50**, 127 (1989).

[34] A.V.Popova, D.K.Hincha. Thermotropic phase behavior and headgroup interactions of the nonbilayer lipids phosphatidylethanolamine and monogalactosyldiacylglycerol in the dry state. BMC Biophysics **1**, 4 (2011).

[35] W.Curatolo. The physical properties of glycolipids. Biochim. Biophys. Acta **906**, 111 (1987).

[36] A.E.Oliver. D.K.Hincha, N.M.Tsvetkova, L.Vigh, J.H.Crowe. The effect of arbutin on membrane integrity during drying is mediated by stabilization of the lamellar phase in the presence of nonbilayer-forming lipids. Chem Phys Lipids **111**, 37 (2001).

[37] N.M.Tsvetkova, I.Horváth, Z.Török, W.F.Wolkers, Z.Balogi, N.Shigapova, L.M.Crowe, F.Tablin, E.Vierling, J.H.Crowe, L.Vigh. Small heat-shock proteins regulate membrane lipid polymorphism. Proc. Natl. Acad. Sci. USA. **99**, 13504 (2002).

[38] V.Castro, S.V.Dvinskikh, G.Widmalm, D.Sandström, A.Maliniak. NMR studies of membranes composed of glycolipids and phospholipids. Biochim Biophys Acta **1768**, 2432 (2007).

[39] A.R.Mansourian, A.P.R.Brain, P.J.Quinn. Intermolecular mixing of saturated and unsaturated galactolipids. Biochem. Soc. Transactions **14**, 738 (1986).

[40] A.Bruno, C.Rossi, G.Marcolongo, A.Di Lena, A.Venzo, C.P.Berrie, D.Corda. Selective in vivo anti-inflammatory action of the galactolipid monogalactosyldiacylglycerol. Eur J Pharmacol **524**, 159 (2005).

[41] N.Maeda, Y.Kokai, S.Ohtani, H.Sahara, Y.Kumamoto-Yonezawa, I.Kuriyama, T.Hada, N.Sato, H.Yoshida, Y.Mizushina. Anti-tumor effect of orally administered spinach glycolipid fraction on implanted cancer cells, colon-26, in mice. Lipids **43**, 741 (2008).

[42] N.Maeda, Y.Kokai, S.Ohtani, H.Sahara, T.Hada, C.Ishimaru, I.Kuriyama, Y.Yonezawa, H.Iijima, H.Yoshida, N.Sato, Y.Mizushina. Anti-tumor effects of the glycolipids fraction from spinach which inhibited DNA polymerase activity. Nutr Cancer **57**, 216 (2007).

[43] I.Kuriyama, K.Musumi, Y.Yonezawa, M.Takemura, N.Maeda, H.Iijima, T.Hada, H.Yoshida, Y.Mizushina. Inhibitory effects of glycolipids fraction from spinach on mammalian DNA polymerase activity and human cancer cell proliferation. J Nutr Biochem. **10**, 594 (2005).

[44] B.S. Chu, A.P.Gunning, G.T. Rich, M.J. Ridout, R.M. Faulks, M.S. Wickham, V.J. Morris, P.J.Wilde. Adsorption of bile salts and pancreatic colipase and lipase onto digalactosyldiacylglycerol and dipalmitoylphosphatidylcholine monolayers. Langmuir **26**, 9782 (2010).

[45] B.Gzyl-Malcher, M.Filek, K.Makyła. Langmuir monolayers of chloroplast membrane lipids. Thin Solid Films **516**, 8844 (2008).

[46] A.Tazi, S.Boussaad, R.M.Leblanc. Atomic force microscopy study of cytochrome f (Cyt f) and mixed monogalactosyldiacylglycerol (MGDG)/Cyt f Langmuir-Blodgett films. Thin Solid Films **353**, 233 (1999).

[47] G.A.Georgiev, S.Ivanova, A.Jordanota, A.Tsanova, V.Getov, M.Dimitrov, Z.Lalchev. Interaction of monogalactosyldiacylglycerol with cytochrome b6f complex in surface films. Biochem. Biophys. Res. Commun. **419**, 648 (2012).

[48] J.Kruk, K.Strzałka, R.M.Leblanc. Monolayer study of plastoquinones, alpha-tocopherol quinone, their hydroquinone forms and their interaction with monogalactosyldiacylglycerol. Charge-transfer complexes in a mixed monolayer. Biochim. Biophys. Acta **1112**, 19 (1992).

[49] M.Filek, B.Gzyl-Malcher, P.Laggner, M.Kriechbaum. Effect of indole-3-acetic acid on surface properties of the wheat plastid lipids. J. Plant. Physiol. **162**, 245 (2005).

[50] L.Shao, V.V.Konka, R.M.Leblanc. Surface Chemistry Studies of Photosystem II. J. Colloid Interface Sci. **215**, 92 (1999).

[51] P.Vitovič, D.P.Nikolelis, T.Hianik. Study of calix [4] resorcinarene–dopamine complexation in mixed phospholipid monolayers formed at the air|water interface. Biochim Biophys Acta **1758**, 1852 (2006).

[52] B.Gzyl-Malcher, M.Zembala, M.Filek. Effect of tocopherol on surface properties of plastid lipids originating from wheat calli cultivated in cadmium presence. Chem Phys Lipids **163**, 74 (2010).

[53] S.Y.Zaitsev, N.A.Kalabina, B.Herrmann, C.Schaefer, V.P.Zubov. A comparative study of the photosystem II membrane proteins with natural lipids in monolayers. Mater Sci Eng C **8**, 519 (1999).

[54] R.G.Cain, N.W.Page, S.Biggs. Force calibration in lateral force microscopy. J.Colloid Interface Sci. **227**, 55 (2000).

[55] J.Hoyo, E.Guaus, J.Torrent-Burgues, F.Sanz. Biomimetic monolayer films of digalactosyldiacylglycerol incorporating plastoquinone. Biochim Biophys Acta **1848**, 134 (2015).

[56] J.Hoyo, E.Guaus, J.Torrent-Burgues, F.Sanz. Biomimetic monolayer films of monogalactosyldiacylglycerol incorporating plastoquinone. J Phys Chem B **119**, 6170 (2015).

[57] P.Toimil, G.Prieto, J.Jr.Miñones, F.Sarmiento. A comparative study of F-DPPC/DPPC mixed monolayers. Influence of subphase temperature on F-DPPC and DPPC monolayers. Phys Chem Chem Phys **12**, 13323 (2010).

[58] H.Yun, Y-W.Choi, N.J.Kim, D.Sohn. Physicochemical properties of phosphatidyl-choline (PC) monolayers with different alkyl chains, at the air/water interface. Bull. Korean Chem. Soc. **24**, 377 (2003).

[59] S.Baoukina, L.Monticelli, H.J.Risselada, S.J.Marrink, D.P.Tieleman. The molecular mechanism of lipid monolayer collapse. Proc. Natl. Acad. Sci. USA **105**, 10803 (2008).

[60] R.A.Ridsdale, N.Palaniyar, F.Possmayer, G.Harauz. Formation of folds and vesicles by dipalmitoylphosphatidylcholine monolayers spread in excess. J Membr Biol **180**, 21 (2001).

[61] J.Ding, I.Doudevski, H.E.Warriner, T.Alig, J.A.Zasadzinski. Nanostructure changes in lung surfactant monolayers induced by interactions between palmitoyloleoylphosphatidylglycerol and surfactant protein B. Langmuir **19**, 1539 (2003).

[62] T.F.Alig, H.E.Warriner, L.Lee, J.A.Zasadzinski. Electrostatic barrier to recovery of dipalmitoylphosphatidylglycerol monolayers after collapse. Biophys J **86**, 897 (2004).

[63] J.Hoyo, E.Guaus, J.Torrent-Burgues, F.Sanz. Electrochemistry of LB films of mixed MGDG:UQ on ITO. Bioelectrochemistry **104**, 26 (2015).

[64] H.Hillebrandt, G.Wiegand, M.Tanaka, E.Sackmann. High Electric Resistance Polymer/Lipid Composite Films on Indium-Tin-Oxide Electrodes. Langmuir **15**, 8451 (1999).

[65] G.Aloisi, L.Becucci, A.Dolfi, M.R.Moncelli, F.Tadini-Buoninsegni, R.Guidelli. Interfacial bioelectrochemistry: assessment and trends. J. Electroanal Chem **504**, 1 (2001).

[66] J.Yang, J. M.Kleijn. Order in phospholipid Langmuir-Blodgett layers and the effect of the electrical potential of the substrate. Biophys J **76**, 323 (1999).